

Observation of Single Metal Nanoparticle Collisions by Open Circuit (Mixed) Potential Changes at an Ultramicroelectrode

Hongjun Zhou,[†] Jun Hui Park,[†] Fu-Ren F. Fan, and Allen J. Bard*

Center for Electrochemistry, Department of Chemistry and Biochemistry, The University of Texas at Austin, Austin, Texas 78712, United States

S Supporting Information

ABSTRACT: Single nanoparticle (NP) collisions were successfully observed by a potentiometric measurement. The open circuit potential (OCP) of a measuring Au ultramicroelectrode (UME) changes when Pt NPs collide with the UME in a hydrazine solution. The OCP change is related to the redox processes, the concentration of particles, particle size, and electrode size. Compared with the amperometric technique, this approach has several advantages: higher sensitivity, simpler apparatus, fewer problems with NP decomposition, and contamination.

We report single nanoparticle (NP) detection based on a potentiometric technique by measuring the open circuit potential (OCP) instead of the current. This not only simplifies the measurement considerably, but also makes it possible to attain an even higher sensitivity to the amount of charge transferred. Previously, we described an amperometric technique that allowed detection of single NP collisions with an ultramicroelectrode (UME) based on electrocatalytic current amplification.^{1–5} In this technique, the measuring UME, for example, an Au disk with a 5 μm radius, was held at a potential where only negligible current flowed because the reaction of interest, the oxidation of hydrazine, was not electrocatalyzed at the Au surface. However when a Pt NP, a good electrocatalyst for this reaction, collided with the electrode, a current was observed, and because of the large amplification effect produced a current in the picoampere (pA) range during its encounter with the electrode.

Following earlier work on measurement of current steps for the collision of Pt NPs with an Au UME in the hydrazine system,² we now report the OCP change that results from injecting a solution of Pt NPs. The OCP of a working electrode is its potential measured versus a reference electrode when no external current flows.⁶ In one set of OCP experiments, Pt NPs with an average radius of ~ 16 nm (Figure S1) were used. The Pt NPs were synthesized by NaBH_4 reduction and ascorbic acid reduction in the presence of sodium citrate as capping agent.⁷ After injection of the Pt NPs, the OCP immediately shifted negatively (downward) as shown in Figure 1A. The OCP changed in the form of a sequence of small, millivolt (mV) steps (Figure 1A inset), easily recognized above the about ± 150 μV noise. We have observed similarly shaped current steps when measuring the current at a constant potential bias,^{1,2} which have been ascribed to the sticking of the Pt NPs on the Au UME after the collision. Before the Pt NPs contact the Au

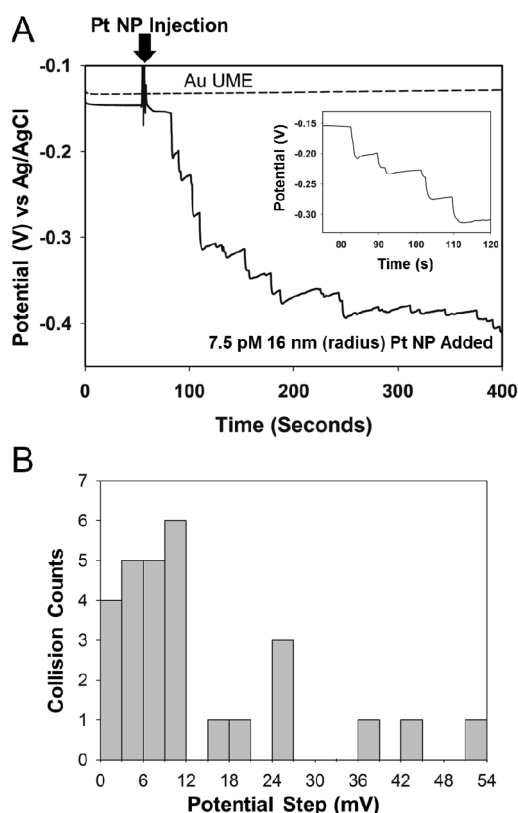


Figure 1. (A) OCP vs time plot for single Pt NP (radius ~ 16 nm) collisions at the Au UME (radius 5 μm) in the presence of 5 mM phosphate buffer (pH 7.0) and 15 mM hydrazine without (dashed line) and with (solid line) 7.5 pM Pt NPs. Inset shows magnified image of staircase potential response. Data acquisition time is 100 ms. (B) Statistical distribution of the number of all recognizable potential steps of different amplitudes (measured over first 340 s after Pt NP injection).

UME, charge transfer can occur between each Pt NP and the solution containing hydrazine to attain a quasi steady state. Similar charge transfer occurs at the Au UME. After the Pt NPs collide and stick to the Au UME, the current balance is changed and a new steady state is established via capacitive charging and the charge transfer reactions between Pt NPs, the Au UME, and redox species as shown schematically in Figure 2A. This causes

Received: June 8, 2012

Published: July 27, 2012

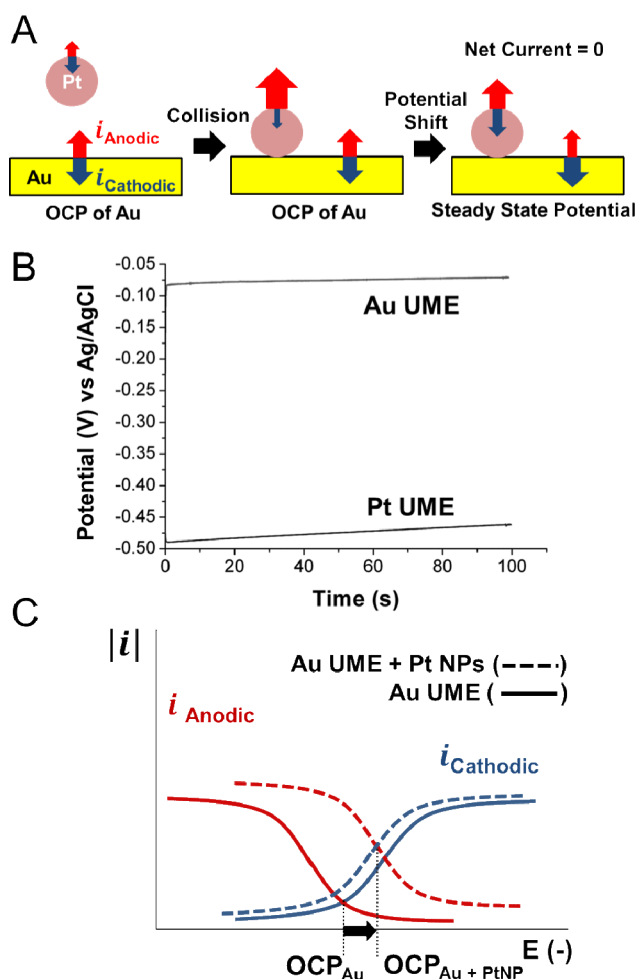


Figure 2. (A) Pictorial representation of the relative changes in the anodic (red arrow) and cathodic (blue arrow) currents on a single Pt NP and on the Au UME before and during particle collision event. (B) OCP of Au and Pt UMEs in a solution of 50 mM phosphate buffer (pH 7.0) and 15 mM hydrazine; radius of Pt and Au UMEs, 5 μm ; sweep rate, 100 mV/s. (C) Schematic representation of the half reaction i - E curves before (solid line) and after (dashed line) a single Pt NP collision event on the Au UME. Note that the currents are absolute values.

a shift in OCP in a sharp transition producing a series of potential steps. The source of the potential decay observed in individual steps is still not clear but may partially be due to surface contamination of the Pt NPs; this slow decay is also observed on a Pt UME (Figure 2B). Potential decay at individual OCP steps is, however, slower than current decay of individual steps with chronoamperometry, as those shown later. Other examples of typical collision curves with 2 nm radius NPs are shown in Figures S2 and S3.

The type of OCP of interest here is not of the reversible or poised type seen with a redox couple,⁸ but one that is kinetically controlled by two or more half-reactions, a so-called *mixed potential*. This situation occurs when there are no oxidized and reduced species of a single half reaction to allow the establishment of a true equilibrium potential, or where the heterogeneous electron transfer rate for a redox couple is very small; such a system is said to be *unpoised*.⁹ Under these circumstances, the potential of the electrode is kinetically established by the position where the overall faradaic current at the electrode is zero. Mixed potential theory was first

established by Wagner and Traud in 1938 and has mainly been of interest in corrosion science.^{10,11} However, the mixed potential concept can be applied more broadly in electrochemistry, for example in treating metal catalysis of solution redox reactions.^{12,13} Moreover, any change of electrode status, for example, deposition/dissolution or adsorption, could cause a change in the mixed potential. Although the concept was initially developed to understand and study corrosion rates,¹⁴ it can be used to study other problems related to electrochemistry, for example, the poisoning effect of arsenic species on Pt electrodes,¹⁵ or the deposition of copper on a Si wafer.¹⁶ So-called mixed potential-based gas sensors for H_2 ,¹⁷ O_2 ,¹⁸ nitrogen oxides,¹⁹ and ammonia²⁰ have also been discussed. We discuss the basic principles of the mixed potential as it is employed here and its sensitivity to small changes elsewhere.²¹

Because the mixed OCP is defined by both the cathodic and anodic half-reaction currents, very small changes in these can result in appreciable changes in the potential. Thus, for example, if an electrocatalytic NP collides and sticks to an inert electrode, it will change the anodic or cathodic half-reaction currents, depending on the reaction catalyzed (e.g., proton reduction or hydrazine oxidation) and this will cause a shift in the potential. Indeed as long as the collision results in some charge transfer with the electrode at open circuit, a potential change will occur.

An illustration of these principles is shown in Figure 2A. Pt is a better electrocatalyst than Au for hydrazine oxidation. Thus, the oxidation onset potential of hydrazine on Pt is ~ 0.4 V less positive than on Au.² The mixed OCP, determined by hydrazine oxidation and reduction of protons and trace amounts of oxygen, also differs by ~ 0.4 V between Au and Pt as shown in Figure 2B. If a Pt NP contacts an Au UME, because of the Pt electrocatalysis of hydrazine oxidation at the OCP of Au, the overall oxidation current on the Pt NP together with that on the Au UME becomes larger than the overall reduction current. To maintain the OCP condition, the OCP shifts negatively to produce a zero net current. Figure 2C illustrates schematically the shift in OCP after a Pt NP collision event on the Au UME with current-potential curves.

The frequency of collisions was monitored at different concentrations of 2 nm radius Pt NPs (Figure 3). At low concentration, the number of steps per unit time was linearly proportional to the NP concentration, indicating that the potential steps are from individual Pt NP collisions. However, at higher concentrations, the number began to deviate from this dependence and was lower than the expected value. This could be caused by the increasing possibility of Pt NP aggregation or by some multiple Pt NP collisions. The distribution of potential steps at high concentration also shows the appearance of more steps of a larger height relative to those observed at low concentration (Figure 3C). The collision frequency (i.e., the number of the recognizable potential steps) calculated at low concentration is about $0.002 \text{ pM}^{-1} \text{ s}^{-1}$, which is lower than the $0.012 \text{ pM}^{-1} \text{ s}^{-1}$ found with current steps under the same conditions.² The difference in frequency may be partially due to the difficulty in counting of all potential steps that are comparable or smaller than the noise level.

As discussed below, an increase in the size of the NPs makes the counting of the number of steps easier and produces a closer agreement of frequency with the amperometric one.

Several control experiments were conducted. We investigated the effect of inverting the electrode and NP compositions. Upon injection of Au NPs (average radius 9 nm, made by the

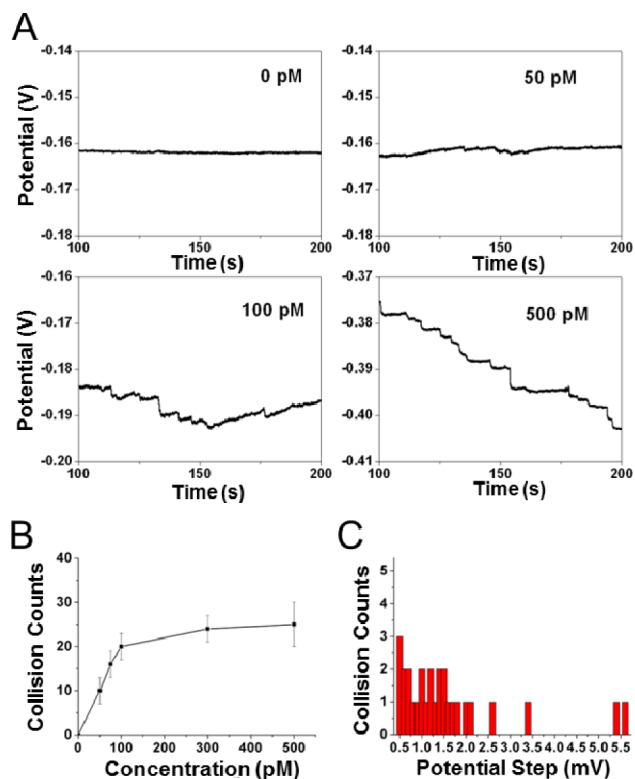


Figure 3. (A) The OCP vs time curves with injected Pt NP (radius ~ 2 nm) at different concentrations at a Au UME radius, $5 \mu\text{m}$. Solution is 50 mM phosphate buffer (pH 7.0) and 15 mM hydrazine under Ar. (B) Total number of recognizable potential steps counted during the time interval of 100 s at different concentrations. (C) Statistical distribution of the number of all recognizable potential steps of different amplitudes at the NP concentration of 500 pM.

citrate reduction method²²) into the solution, the potential versus time curve (Figure S4A) did not show the steps observed in Figure S2. However, a close look (Figure S4C) revealed some transient peaks different from background. The peaks were directed toward more positive potentials (upward). This is consistent with the OCPs of pure Au and Pt UMEs shown in Figure 2B. The potential change depends strongly on the ratio of electrode sizes (e.g., Pt vs Au). In Figure S5, we show the collision behavior of 2 nm radius Pt NPs on a Au UME (radius, $12.5 \mu\text{m}$ rather than the $5 \mu\text{m}$ radius in Figure 3). Instead of potential steps, a continuous shift of potential was observed, indicating a smaller signal from each single NP. When no hydrazine was added to the solution, no change of OCP was observed (Figure S6).

One can contrast the behavior of the 2 nm radius (Figures 3, S2 and S3) and the 16 nm radius Pt NPs (Figures 1, 4, and 5). For the larger NPs, a sequence of potential steps of different amplitudes, ranging from a few to a few tens of mV, can be seen. The statistical distribution of the number of all recognizable potential steps of different amplitudes is shown in Figure 1B. Compared with current steps (an amperometric collision system), which ideally show regular current steps when the particles on the electrodes are far apart, potential steps show a large deviation due to an intrinsic complexity of the potential signal in the mixed potential system. As shown in Figure 1A, the potential steps gradually get smaller after a series of collision events at an Au UME as the OCP approaches that of Pt (in the absence of particle aggregation). The collision

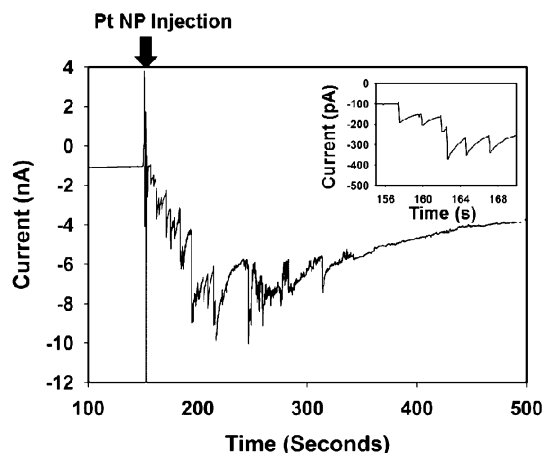


Figure 4. Chronoamperometric curve for single Pt NP (radius ~ 16 nm) collisions at the Au UME (radius $5 \mu\text{m}$) in the presence of 25 mM phosphate buffer (pH 7.0) and 15 mM hydrazine with 7.5 pM Pt NPs. Data acquisition time is 50 ms. Applied potential is -50 mV (vs Ag/AgCl).

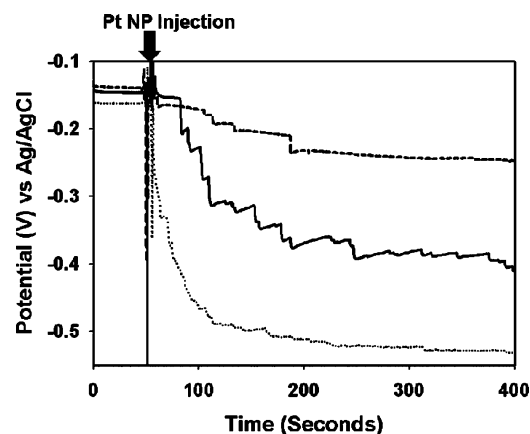


Figure 5. (OCP vs time) plots for single Pt NP (radius ~ 16 nm) collisions at the Au UME (radius $5 \mu\text{m}$) in the presence of 5 mM phosphate buffer (pH 7.0) and 15 mM hydrazine containing various concentration of Pt NPs 2.5 pM (dashed line), 7.5 pM (solid line), and 15 pM of Pt NPs. Data acquisition time is 100 ms.

frequency calculated from Figure 1A is about $0.011 \text{ pM}^{-1} \text{ s}^{-1}$. Note that in this case the chronoamperometric determination of collision frequency at the same Au UME with the same particle concentration gives a comparable estimate of the collision frequency of ca. $0.015 \text{ pM}^{-1} \text{ s}^{-1}$ (see Figure 4), although the current decays with time in the long time regime because of deactivation processes as reported previously.²

As with the 2 nm radius Pt NPs, the OCP versus time curves at a Au UME for 16 nm radius Pt NPs also depend on the concentration (Figure 5). The OCP reaches a nearly constant steady-state value in the time range recorded (≤ 400 s); these are nearly proportional to the concentration of Pt NPs in the concentration range 1–15 pM. Injection of higher concentrations of Pt NPs does not result in more negative steady-state OCPs, because the OCP of Pt (~ -0.5 V as shown in Figure 2B) has already been attained with 15 pM Pt NPs. Rather there is an immediate potential shift from the OCP of Au to the OCP of Pt with injection of higher concentrations of Pt NPs (Figure S7). On the basis of the OCP change from Au to Pt over a time series of countable number of potential steps, we conclude that

only a fraction of the Pt NPs stick to the Au UME. In general, the OCP detection method appears to be more sensitive to small particle detection than the amperometric one.

To mimic the particle collision experiment, we carried out experiments in which the OCP of Pt UMEs of different sizes was measured alone and when connected to an Au UME. The results showed analogous behavior to the OCP changes observed in particle collision experiments. These results will be reported elsewhere with the theoretical treatment.²¹

In summary, we present a potentiometric technique for single NP collision experiments (Pt NP/Au UME/hydrazine oxidation). The OCP change is related to the size of the UME, the NPs, and the concentration of hydrazine. The potential steps corresponding to single Pt NP sticking were observed by measuring OCP versus time. Our results indicate that the OCP change may be used as a sensitive technique for single NP detection. Compared with the amperometric technique, it has the advantage of simpler apparatus, higher sensitivity, and less problems associated with NP deactivation. Further work for a more quantitative evaluation and analysis of the OCP response with and without a mediator and estimation of the extremely small charge exchanged between two conductive materials during contact will be reported.

■ ASSOCIATED CONTENT

🔗 Supporting Information

Experimental procedures and additional experimental results. This material is available free of charge via the Internet at <http://pubs.acs.org>.

■ AUTHOR INFORMATION

Corresponding Author

ajbard@mail.utexas.edu

Author Contributions

†These authors contributed equally.

Notes

The authors declare no competing financial interest.

■ ACKNOWLEDGMENTS

The support of this research by The UT Center for Electrochemistry and the National Science Foundation (CHE-1111518) are gratefully acknowledged.

■ REFERENCES

- (1) Xiao, X.; Bard, A. J. *J. Am. Chem. Soc.* **2007**, *129*, 9610–9612.
- (2) Xiao, X.; Fan, F.-R. F.; Zhou, J.; Bard, A. J. *J. Am. Chem. Soc.* **2008**, *130*, 16669–16677.
- (3) Kwon, S. J.; Fan, F.-R. F.; Bard, A. J. *J. Am. Chem. Soc.* **2010**, *132*, 13165–13167.
- (4) Zhou, H.; Fan, F.-R. F.; Bard, A. J. *J. Phys. Chem. Lett.* **2010**, *1*, 2671–2674.
- (5) Bard, A. J.; Zhou, H.; Kwon, S. J. *Isr. J. Chem.* **2010**, *50*, 267–276.
- (6) In reality, during the measurement of the OCP with an electrometer, a very small current flows, depending on the input impedance of the measuring device, which can be as large as 200 TΩ.
- (7) Bigall, N. C.; Härtling, T.; Klose, M.; Simon, P.; Eng, L. M.; Eychmüller, A. *Nano Lett.* **2008**, *8*, 4588–4592.
- (8) The reversible OCP, the same as the nernstian potential or equilibrium redox potential, is governed by the activities of species in solution or on the electrode surface and is a measure of the thermodynamics of the reversible half reaction at the electrode surface. In this case, the electrode is said to be *poised* at the reversible potential.
- (9) Poised and unpoised systems in electron transfer are analogous to buffered and unbuffered systems in acid/base chemistry.

- (10) Wagner, V. C.; Traud, W. Z. *Elektrochem.* **1938**, *44*, 391–402.
- (11) Wagner, V. C.; Traud, W. *Corrosion* **2006**, *62*, 843–855.
- (12) Spiro, M. J. *Chem. Soc., Faraday Trans. 1* **1979**, *75*, 1507–1512 and references therein.
- (13) Miller, D. S.; Bard, A. J.; McLendon, G.; Ferguson, J. J. *Am. Chem. Soc.* **1981**, *103*, 5336–5341.
- (14) Zelinsky, A. G.; Pirogov, B. Y.; Yurjev, O. A. *Corros. Sci.* **2004**, *46*, 1083–1093.
- (15) Gao, L. J.; Conway, B. E. *J. Electroanal. Chem.* **1995**, *395*, 261–271.
- (16) Parkhutik, V.; Rayon, E.; Pastor, E.; Matveeva, E.; Sasano, J.; Ogata, Y. *Phys. Status Solidi* **2005**, *202*, 1586–1591.
- (17) Sekhar, P. K.; Brosha, E. L.; Mukundan, R.; Nelson, M. A.; Williamson, T. L.; Garzon, F. H. *Sens. Actuators, B* **2010**, *148*, 469–477.
- (18) Vallieres, C.; Gray, J.; Poncin, S.; Matlosz, M. *Electroanalysis* **1998**, *10*, 191–197.
- (19) Lu, G.; Miura, N.; Yamazoe, N. *J. Mater. Chem.* **1997**, *7*, 1445–1449.
- (20) Schonauer, D.; Wiesner, K.; Fleischer, M.; Moos, R. *Sens. Actuators, B* **2009**, *140*, 585–590.
- (21) Zhou, H.; Fan, F.-R. F.; Park, J. H.; Zhang, B.; Bard, A. J. In preparation.
- (22) Frens, G. *Nat. Phys. Sci.* **1973**, *241*, 20–22.